

Successful Starshade Petal Deployment Tolerance Verification in Support of NASA's technology development for exoplanet missions

D. Webb^b, N. J. Kasdin^a, D. Lisman^b, S. Shaklan^b, M. Thomson^b, E. Cady^b, G. W. Marks^c,
A. Lo^c

^aPrinceton University, Princeton, NJ, 08544 USA

^bJet Propulsion Laboratory, California Institute of Technology, Pasadena, CA, 91109 USA

^cNorthrop Grumman Aerospace Systems, Los Angeles, CA, USA

ABSTRACT

A Starshade is a sunflower-shaped satellite with a large inner disk structure surrounded by petals that flies in formation with a space-borne telescope, creating a deep shadow around the telescope over a broad spectral band to permit nearby exoplanets to be viewed. Removing extraneous starlight before it enters the observatory optics greatly loosens the tolerances on the telescope and instrument that comprise the optical system, but the nature of the Starshade dictates a large deployable structure capable of deploying to a very precise shape. These shape requirements break down into key mechanical requirements, which include the rigid-body position and orientation of each of the petals that ring the periphery of the Starshade. To verify our capability to meet these requirements, we modified an existing flight-like Astromesh reflector, provided by Northrop Grumman, as the base ring to which the petals attach. The integrated system, including 4 of the 30 flight-like subscale petals, truss, connecting spokes and central hub, was deployed tens of times in a flight-like manner using a gravity compensation system. After each deployment, discrete points in prescribed locations covering the petals and truss were measured using a highly-accurate laser tracker system. These measurements were then compared against the mechanical requirements, and the as-measured data shows deployment accuracy well within our milestone requirements and resulting in a contrast ratio consistent with exoplanet detection and characterization.

Keywords: External occulters, occulters, Starshades, exoplanets, high-contrast imaging, TDEM

1. INTRODUCTION

This paper describes a recent technology demonstration toward a Starshade concept for imaging exoplanets that was performed under NASA's Technology Development for Exoplanet Missions (TDEM) funding. As a space based mission designed to image exoplanets, Starshade has several advantages including reduced requirements on the companion telescope, ability to image close in planets with reasonable apertures, however Starshade has its own challenges including large structures with precision shapes. Previous work under this funding showed the ability to manufacture and verify flight-like occulter petals of the required shape for an external occulter design. In this demonstration we demonstrated the capability to place those Starshade petals in the correct location and orientation such that we would have an as-deployed Starshade capable of imaging exoplanets. It should be noted that our approach for designing the Starshade occulter uses optimization tools that result in a smaller occulter size while still obtaining the require starlight suppression over a the desired spectral band, which translates into tighter mechanical tolerances. We took this approach because larger Starshades are increasingly difficult to manufacture, fit into a launch fairing and to verify and test, despite the relaxed tolerances.

The white paper for our TDEM describes in detail our technology milestone, however I have repeated the milestone statement below:

- Verify that the deviations of the petal base point from the design circle are repeatedly below the 3 sigma positioning requirement for a 10^{-9} contrast using a sufficient number of deployments to verify the requirements are met with 90% confidence.

Given the unprecedented nature of the development, we chose a milestone of 10^{-9} because it resulted in a relaxed requirement for the positional accuracy and repeatability of the petal root positions that still represented the ability meet real size goals. Our hope was to do much better than this and discover through this TDEM how to greatly improve our mechanical design such that we could reach higher levels of contrast through tighter performance tolerances. The chosen contrast for our milestone resulted in a deployed petal root positional deployment accuracy requirement of ± 0.95 mm for each of the two petal roots at the base of each petal. We were able to achieve this accuracy at 90% confidence over 15 partial stow and deploy cycles.

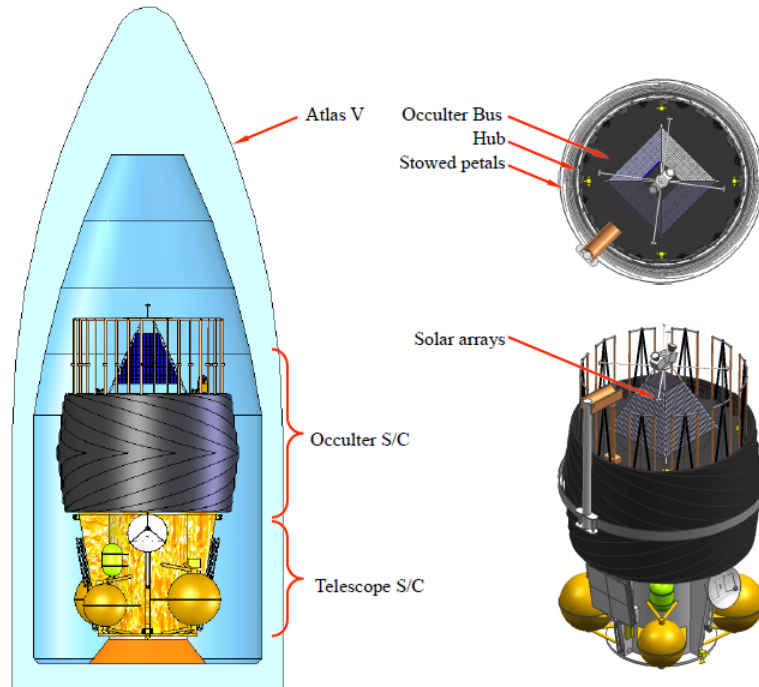


Figure 1. External occulter in fairing, launch configuration



Figure 2. Starshade petal unfurling sequence

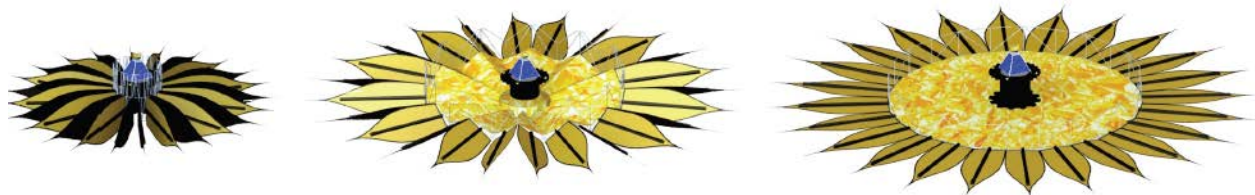


Figure 3. Starshade inner disk truss deployment sequence

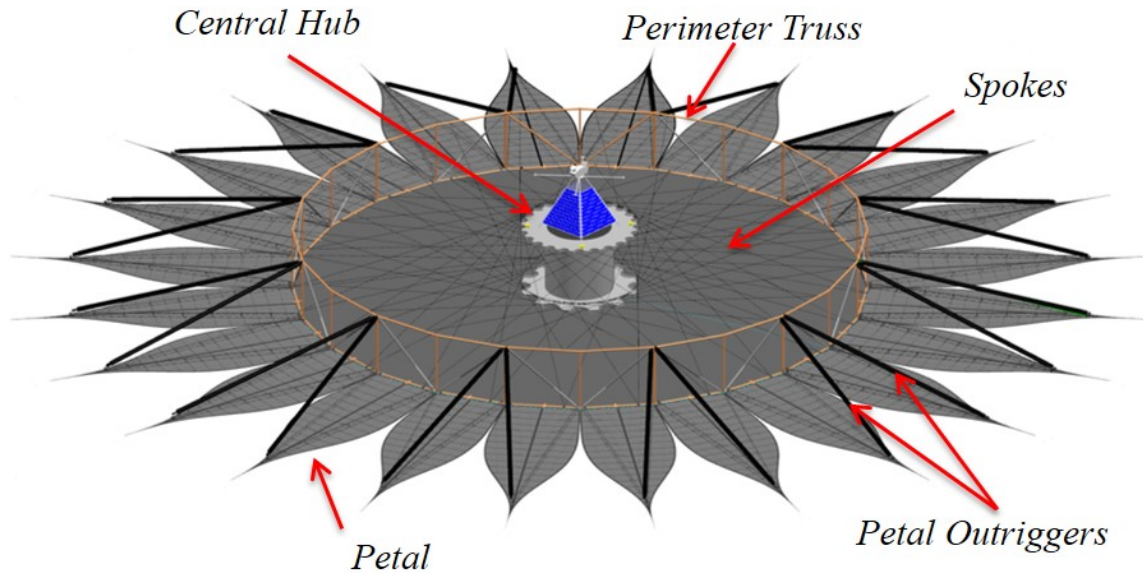


Figure 4. Starshade principle components

2. EXPERIMENT DESIGN OVERVIEW

Given the intent of verifying petal root positional accuracy, our goal was to simulate the conditions most relevant to a flight-like system in order to validate our test. This meant our test Starshade needed to contain all the relevant components and assemblies from our Starshade baseline architecture in Figure 4. The architecture of the Starshade is similar to a bicycle wheel, with tensioned spokes connecting a central hub to the out rim, to which we attach petals. Because our petal roots are the component of interest and must be positioned accurately and repeatedly deployed, it makes sense that the petal root positions be very closely related to the most stable points on the truss, the truss node, to which the spokes attach and connect the truss stiffly back to the central hub. Additional out of plane stiffness is added to the petals by connecting the petal tips back to the truss as well via a component called an outrigger. This meant that our test setup needed to include petals, a truss, petal outriggers, spokes, a hub and gravity offloading system to allow the Starshade to deploy in a space like environment. The components and assemblies used in our test setup are shown in Figure 5 and described in the next section.

In order to validate our petal root deployment accuracy capability, we needed a system to measure each of the petal roots for absolute position for each deployment as well as a number of other positions on the truss in order to capture the overall repeatability of deployment of the truss nodes, the stable points of the truss. We chose to use a combination of photogrammetry and laser tracker. We would end up primarily relying on the laser tracker based on the test environment. More detail of the data collection process and analysis are described later in the paper.

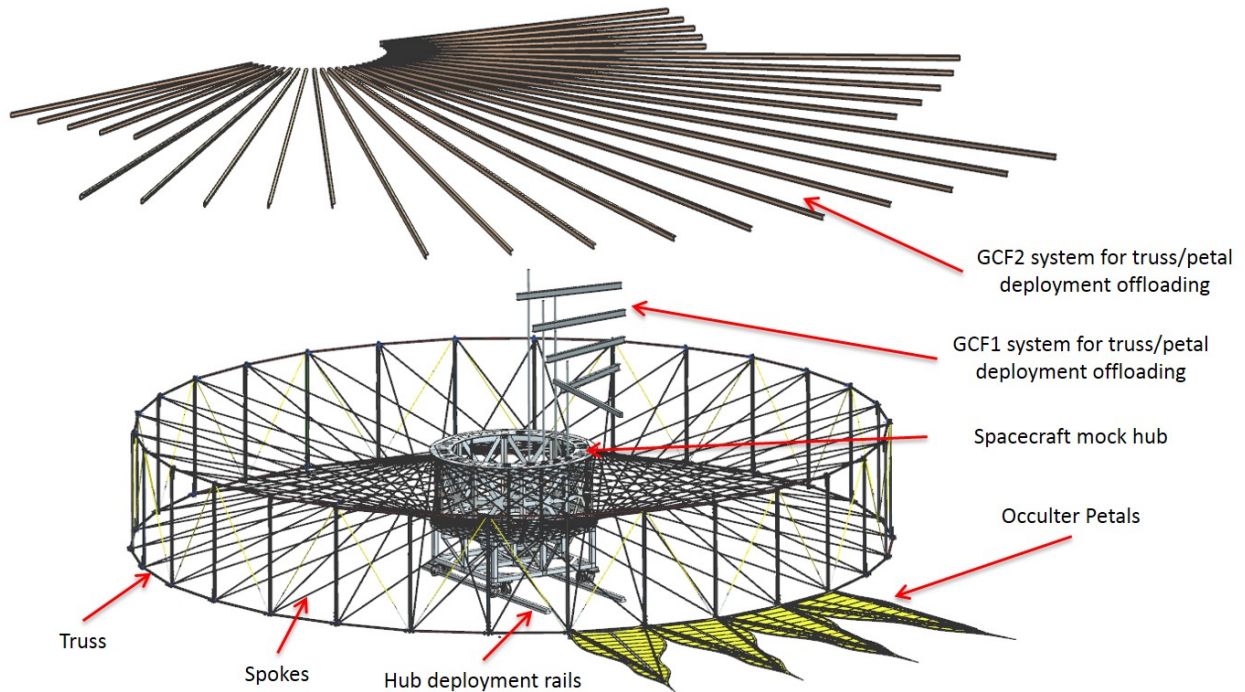


Figure 5. Starshade deployment tolerance test setup with gravity offloading systems

3. EXPERIMENT MECHANICAL DESIGN

3.1 **Hub Design and Manufacture.** The central hub shown in Figures 5 & 6. provides a stiff body, emulative of the condition we will have in flight, from which to deploy the truss and petals. The hub was designed by Northrup Grumman Aerospace Systems (NGAS), Carpinteria, with high level requirements from JPL. The design allows 120 truss spokes to attach tangentially from the two parallel discs at the top and bottom of the hub to the individual nodes of the truss. This bicycle wheel spoke design, from central hub to truss, creates a stiff structure to which we attached our Starshade petals. The hub was designed to have interfaces for features that allow the truss to collapse and stow around its outer perimeter. The petals then furl around the truss/hub system and mount against mounting hardware that protrudes from the hub and through the truss. Additional gravity compensation fixture hardware (GCF1) designed by JPL, offloads the weight of the petals during the unfurling stage of the deployment. The central hub, hub deployment rails and petal attachment points were fabricated by NGAS.

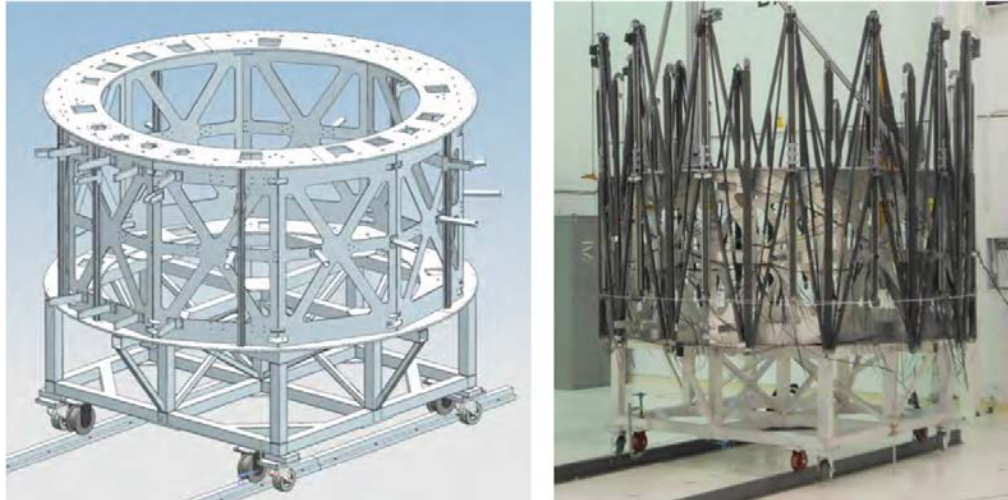


Figure 6. As-built hub with Astromesh truss stowed around it

3.2 **Petal Design and Manufacture.** A critical component of the deployment positioning and repeatability requirement, the Starshade petals were constructed in the summer of 2012 over a ten week period by two Princeton and two MIT undergraduate summer students. The Starshade petals consist of a center spine, or backbone, a base spine to interface to the truss and structural edges to which the optical edges attach. The structural edges are tied back to the center spine via the battens and the whole structure is given shear stiffness from the longerons. In order for the entire petal to wrap around the spacecraft, a flexible material was used as the core of the petal center spine. This unique design allows for the petal to be flexible enough to furl around a 3-meter spacecraft hub and also passively become rigid as the petal unfurls and a pair of spring loaded ribs deploy and rigidize the petal. A schematic of the petal design (the same is in our first TDEM) is shown in Figure 7. and the completed as-built petals are shown in Figure 8. Attached to the NGAS truss.

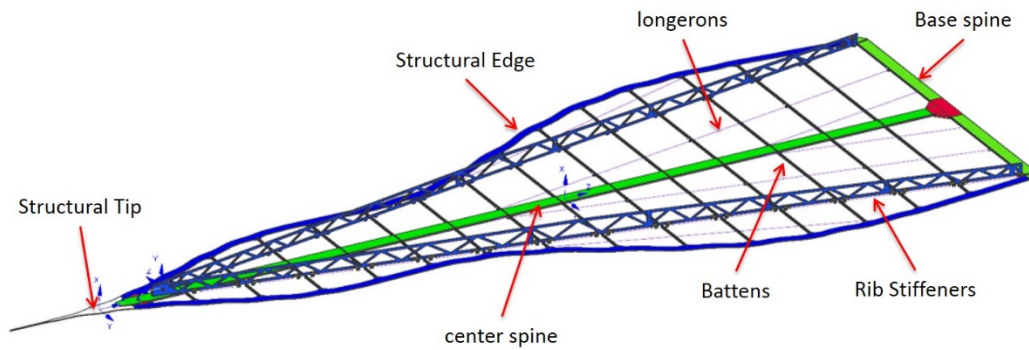


Figure 7. Petal main components

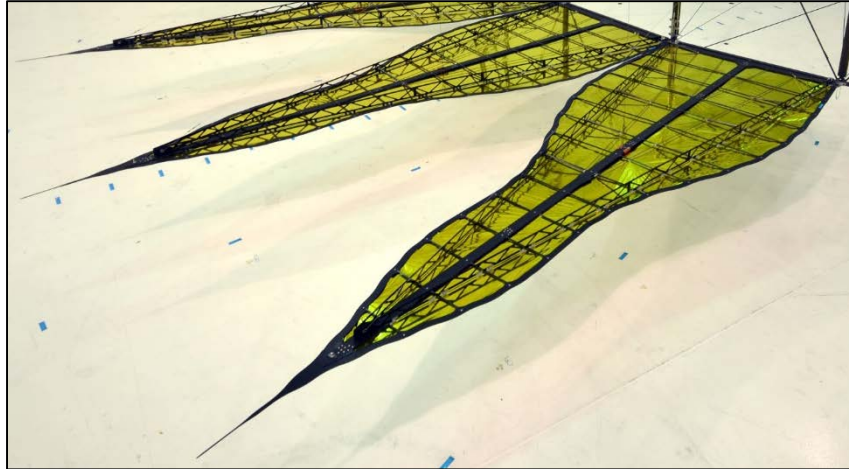


Figure 8. Petals as-built and installed on deployed truss

3.3 Petal-Truss Interface Design and Manufacture. The petals mount to the truss longerons with precision pinned joints. The deployment tolerance milestone applies to the petal attachment points and more specifically, the center of each interface joint. This center point was precisely characterized relative to petal mounted targets using photogrammetry. Figure 9. Shows the petal interfaces with respect to the truss nodes as well as prime and dependent truss nodes relative to the petal positions. The design of the Northrup Grumman truss was not commensurate with a petal to longeron interface that would allow furling of the petals around the truss in the stowed condition. For this reason, the fittings that were used to attach the petals to the truss were designed to meet the requirement of quick and repeatable detachment of the petal from the truss longerons via a quick release style fitting that was also designed to maintain the position of the petals with respect to the truss with great precision. Also designed into the petal-to-truss interface fitting is the ability to shim the petal in the truss radial direction, allowing us to correct for absolute radial position error of the petals after our first set of measurements. The interface fitting consists of two pieces, one that is permanently attached to the truss and the other that is attached to the petal via the quick release mechanism already mentioned. Repeatability of the petal position pre- to post-shimming was maintained via registration features between the two parts of the fitting; this allowed repeatability over an order of magnitude better than our requirement.

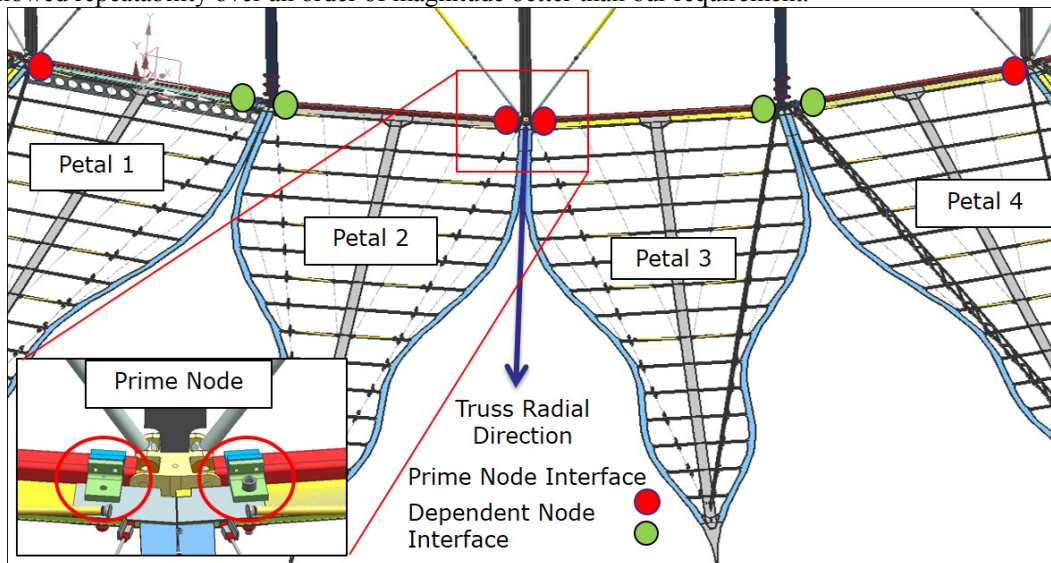


Figure 9. Petal interface points with respect to truss prime and dependent nodes. Dots represent petal interfaces with color indicating type

Placing the petal interface fittings with the required precision to meet the milestone required a tool that would repeatedly place each petals interface fittings with respect to known locations on the truss. The tool that was used to place the petal-to-truss interface fittings was a single piece and was the same tool that was used for placing the petal interfaces into the petal base spine to which the petal-truss fitting connected. Placement of the petals with respect to known locations on the truss requires a truss that has known and repeated features at each bay of the truss to which the petal placement tool can be referenced. In our case this was a challenge as the truss was not designed with any known and repeated features to which we could reference and only every other node of the truss was identical. An additional challenge was that the truss model available to us was later found to vary from the as-built prototype. Because only every other node of the truss was identical, this created mirror image bay pairs to which we were only able to reliably place pairs of petals that were symmetric about the node that contained the reliable feature to which we could reference. This node that contained reliable features is referred to as the prime node, which in our case was centered on the inner two of the four petals. The node that was not referenced for tangential positioning of the petals is referred to as the dependent node. Because of this, the two outer petals referenced prime nodes that were the second node removed from the reference point of the two inner petals. This meant that the two outer petals could not be well related tangentially to the two inner petals. This relationship can be seen in Figure 9.

3.4 Truss Spokes. With the given position repeatability requirements for the petal root points, it was critical to create a very stiff connection from the petal roots back to the very stiff central hub structure. This was accomplished via a very stiff spoke that connected the nodes of the truss, to which the petal roots were very well coupled, and that was flexible when not tensioned so as to allow for easy stowing. The stiffness and thus repeatability of the system was achieved by choosing a material that was very low strain, thus reducing deflection and increasing repeatability. These spokes were also very thermally stable, which in our case was important not only for flight but also for testing, due to the very high precision required for the petal root positions. A challenge encountered in using these spokes was managing the long lengths of each of the 120 spokes during truss deployment such that the spokes would not catch on any of the truss or hub features and break. This was very important in that even one broken spoke could be responsible for changing the overall position of the petals. This required designing a spoke deployment method that controlled the spokes during deployment such that incremental lengths of the spokes were released as the truss deployed. This was accomplished with numerous small spring-like restraints that constrained the length of the spoke. Lower resistance restraint springs were used on the length of the spring near the truss connection and increasing resistance was used as the spoke approached the hub. This resulted in a very robust spoke deployment system that constrained determinant lengths of the spokes to release from their restraints only as the deploying truss tugged them out of their restraints.



Figure 10. Spokes uncontrolled on floor, before spoke restraint system

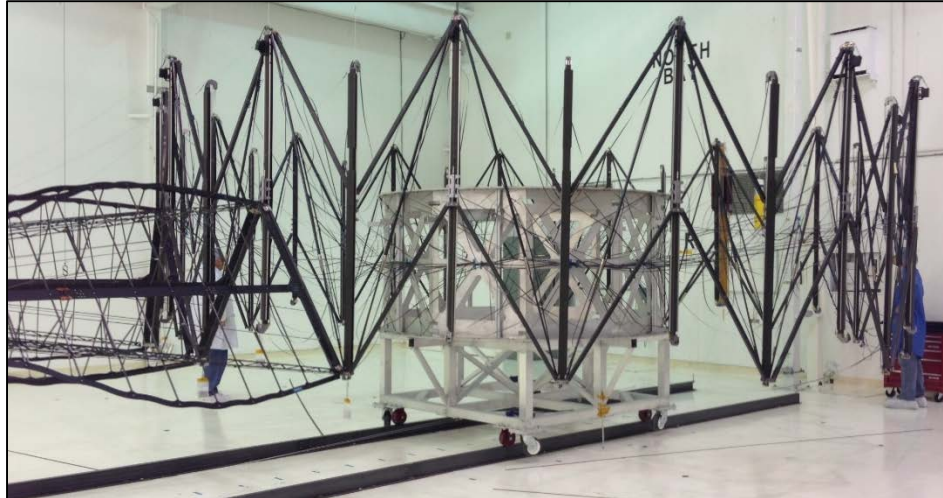


Figure 11. Spoke restraint system implemented, spokes remain taut and controlled throughout deployment

4. DEPLOYMENTS AND METROLOGY

4.1 **Initial Shimming and Metrology.** The initial metrology plan called (described in our milestone whitepaper) for the use of photogrammetry to measure absolute positions at the roots of the petals as well as a number of points spread over each petal and the entire truss. With many points all over the truss and petals, this would give us many data points to determine the repeatability of the truss deployment. Additionally, a laser tracker, referenced to a few points, was also used for comparison, though the number of corner cubes applied was relatively small compared to the number of photogrammetry targets placed all over the truss, hub, and petals. We in fact used both for the initial estimates of the petal positioning before shimming. After completing pre-shim data analysis, however, it was found that the precision of the photogrammetry system was strongly dependent on target position on the occulter, a fact attributed to the geometry of the test facility used for the deployment. The pre-shim data analysis measurements showed that the laser was able to provide more accurate results for our specific location, as photogrammetry requires large angle triangulation, which was not available in our space constrained test area. Moreover, the precision of the laser tracker was uniformly better than the photogrammetry system



Figure 12. Petals on truss, ready to deploy

Once it was determined that the laser tracker was more accurate, the laser tracker was used for the shim installation, post-shim data collection, and to measure the 8 petal root points as well as 42 other points on the truss nodes during deployment. Verification of the accuracy of each laser tracker measurement was

performed by measuring each of the 50 points sequentially a total of three times and then comparing these measurements. If one measurement read an error, that measurement was compared to the other two measurements from the same deployment, and if those were in agreement and the initial erroneous, the erroneous measurement was removed. The laser tracker setup with respect to the Starshade system and the measured locations can be seen on the fully deployed system in Figure 13.

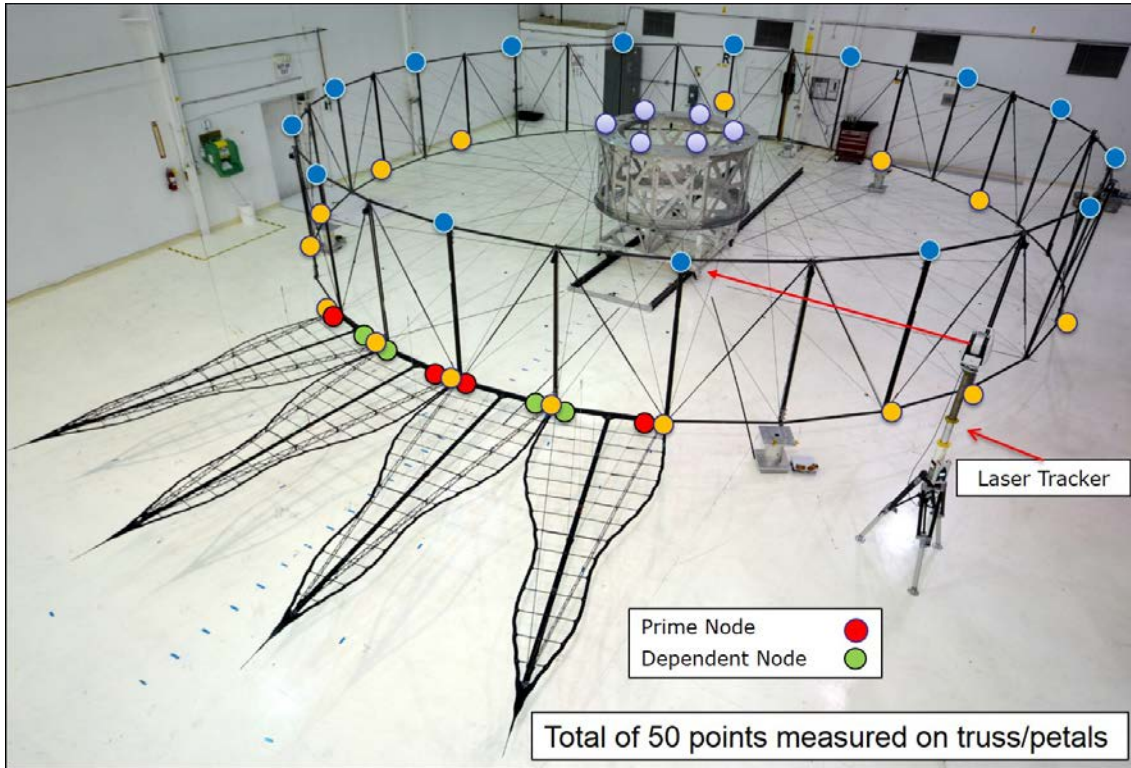


Figure 13. Metrology configuration, dots indicate location measured, color indicates type

To shim the petals, a fit was performed to a set of model points using the procedures outlined later in Section 7.2. The differences, all less than 0.25 mm, were taken out manually in the radial direction with known shim increments at the petal-to-truss interface fitting (The architecture did not allow shimming in the tangential direction.) This proved effective; a post-shim measurement showed that the mean offset from the model in the radial direction decreased from 0.151 mm to 0.063 mm. The tangential direction remained virtually unaltered as expected, with a mean difference of 0.016 mm between before- and after-shim model offsets. Figure 14 shows both of these cases.

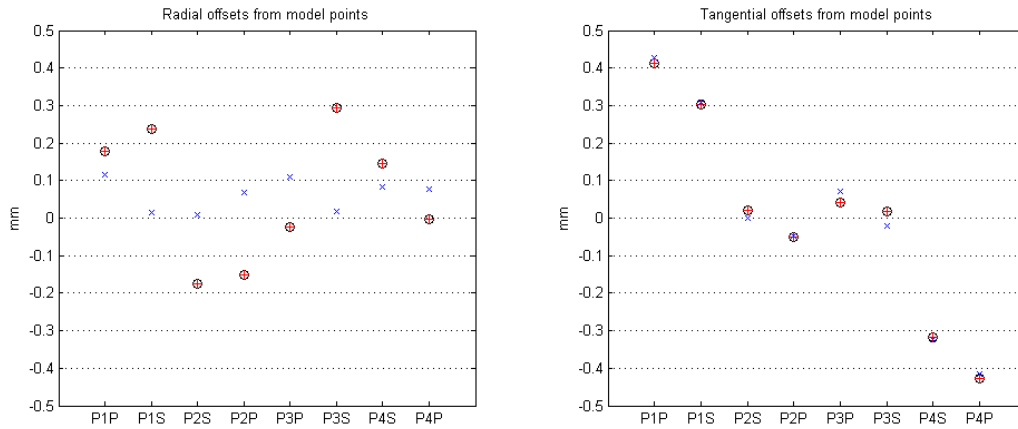


Figure 14. Offsets between data model points before and after shimming. Pre-shim points are designated with black circles with red crosses and post-shim points with blue X's. *Left.* Radial Direction (shimmed) *Right.* Tangential direction (not shimmed)

4.2 Partial Deployments. Initial plans called for furling the petals around the stowed truss between some of the deployments. However, because the gravity compensation system for furling the petals around the truss required a large structure mounted to the top of the hub that contained swinging rails that would rotate across the truss deployment path, it was determined that mounting this hardware to the hub before taking deployment data posed several risks. First it was possible to damage the truss while mounting the hardware on top of the hub, a procedure that could only be performed after the hub was inside the truss structure. Additionally, there was a concern that detaching all the necessary truss gravity offloader lines would be extremely time consuming, posing a risk to achieving the number of deployments required to achieve 90% confidence. Additionally, upon reviewing the petal interface to the truss, it was determined that petal furling would not contribute to any change in the petal root position points that were being measured, as the base spines were registered to stiff fittings that were firmly inserted into petal base spine and thus would not be affected by furling. Another reason for furling the petals would be to determine the effect of petal furling on the truss longerons. Because the existing truss design did not allow us to leave the petals attached to the truss longerons for stowing, but rather we had to detach the petals completely from the truss, the petals could not impart loads on the longerons during furling. For these reasons, no measurable gain would be realized in furling the petals between deployments. The petal unfurling gravity offloader hardware can be seen in Figure 15.



Figure 15. Petal unfurling sequence and unfurling GCF shown crossing stowed truss offloaders

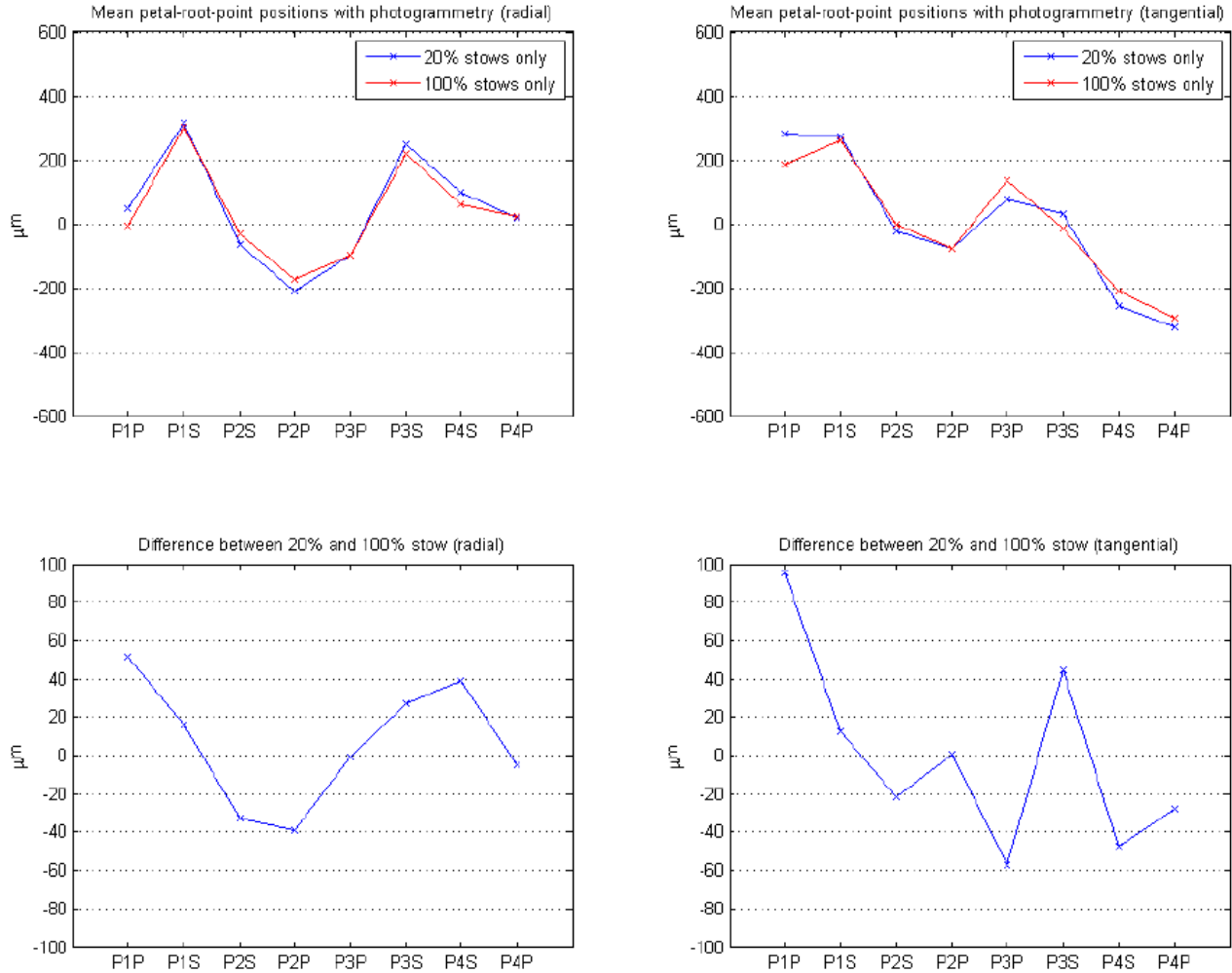


Figure 16. *Top.* Mean locations for the petal root points with partial stows (20% stowed) and full stows (100% stowed), in radial and tangential directions. *Bottom.* Differences between the partial- and full-stow cases. Unlike the data in the rest of the figures in this report, this data was taken with a photogrammetry system rather than a laser tracker. With the exception of the P1P point in the tangential direction, all differences are within the ± 75 micrometer error bars of the photogrammetry system.

5. PROCESSING AND ANALYSIS

The final tests occurred in October, 2013 at the Northrop Grumman Aerospace Systems (NGAS) Astromesh production facility in Goleta, CA. Based on the 10 deployments with metrology performed in August 2013 to determine petal shimming amounts, 15 partial stow and deploy cycles were completed to verify the milestone in October to verify the milestone. Figure 13. shows a picture of the fully deployed truss with petals attached.

5.1 **Data collection.** The final set of data consists of 16 deployments: an initial re-deployment following the installation of the radial shims, and 15 stow-and-deploy cycles on the same day as the initial re-deployment and the two subsequent days. These cycles were a mixture of 10 10%-stows and 5 50%-stows, with the stow percentage representing roughly the fraction of the total radial motion of the truss which was exercised. During the initial photogrammetry tests, 7 20%-stows were taken along with 3 100%-stows. The mean locations of the petal root points were examined for both the partial and full-stow cases, and the residual differences in the locations of the resulting data points, shown in Figure 16, were found to be of comparable order to the 75 micrometer position-error specification for the V-STARS system. Given the longer periods of time required for the full stow (3 hours or more, compared to 30 minutes for a 50%-stow and 10 minutes for a 10%-stow), we

decided to use a mixture of partial stows only in the post-shim testing. A listing of the data sets is given in Table 1.

5.2 Data processing. Each data set consists of three subsets which were taken in immediate succession without moving the deployed occulter. We expect, since the occulter was not moved between the three 45-second-long data collections, that these points should be identical except for the small random measurement error of the laser tracker, and for the most part this is true. However, there are occasionally strong outliers in a single data point from one of the three sets, which introduce nontrivial deviations in the locations of the measured points if the means of the three subsets are used. To avoid these deviations (which given the correspondence between the measured positions in the other two subsets, we believe to be nonphysical) we instead use the median of the three subsets as the canonical data value for that set. To co-fit the separate deployments, all 16 deployment datasets are placed into a single nonlinear least-square fit, which translates and rotates each of the 16 sets of data as a rigid body to co-align them. (As it is unreferenced to external fixed points, the resulting coordinate system is only unique up to a constant global translation and rotation, but this gauge transformation does not affect our analysis.) Not all of the data points are used for this fit, however. The rigid structure of the hub is not perfectly coupled to the truss, and neither are the petal tips. We exclude these points from the truss co-alignment fit, though we do apply the resulting coordinate transforms to look at the spreads of hub and petal-tip points.

Conversely, no other point (hub and petals included) was excepted from further analysis. Data quality was not used as a metric for excluding points; while some points appear suspect based on the data spread (e.g. HUB2, PTR8), we did not exclude them without a corresponding physical explanation for their excision. After the deployments are aligned to each other, we extract the points located at nodes at the root of each petal. These nodes are also present in a CAD model of the system, falling on a circle, and the locations of these nodes in the model were also extracted; the two were then fit against each other to determine the correspondence between measured and model points. The milestone specification called for a fit to a best-fit circle rather than points extracted from a structural model of the system. However, using explicit points in a model in the fit provides two primary advantages:

- (1) Using points derived from a model provides traceability between desired and measured locations for the nodes.
- (2) The coordinate system of the model is chosen such that the center of the model coincides with the origin, and so the vectors between the measured and model points may be projected into radial (directly outward from origin) and tangential (perpendicular to radial) directions. Given this, we can constrain the alignment of the petal root points in a tangential direction. With a best-fit circle, as originally suggested in our white paper, no such constraints can be placed. Figures 17 & 18 show the spread of the laser-tracker positions over the 16 deployments. As we have a set of coordinate transformations which take each of the 16 sets of data into a coordinate system with the model center of the truss at the origin, we have transformed them into radial and tangential coordinates as well. Note, these are deviations from each points mean only.

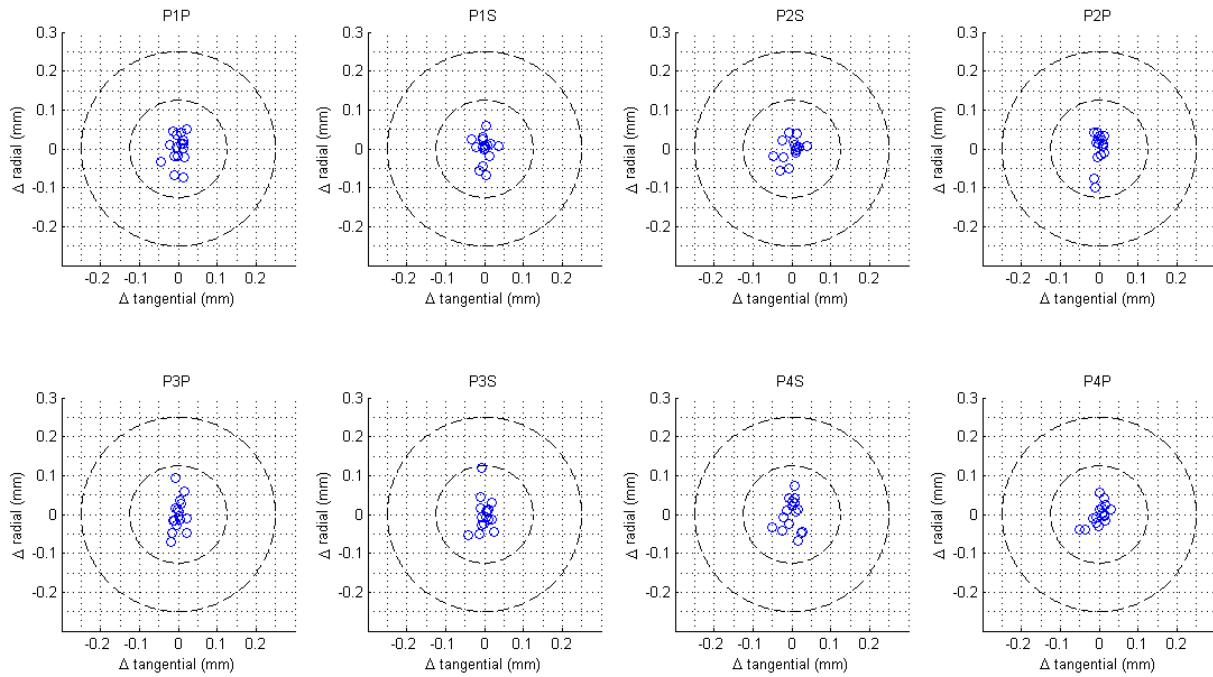


Figure 17. The spread of petal root points over the 16 deployments. Radial and tangential directions are the (r, theta) unit vectors in a polar coordinate system with the nominal occulter center at the origin. Blue circles represent individual deployments. Circles of radius 125 micrometers and 250 micrometers are shown for scale.

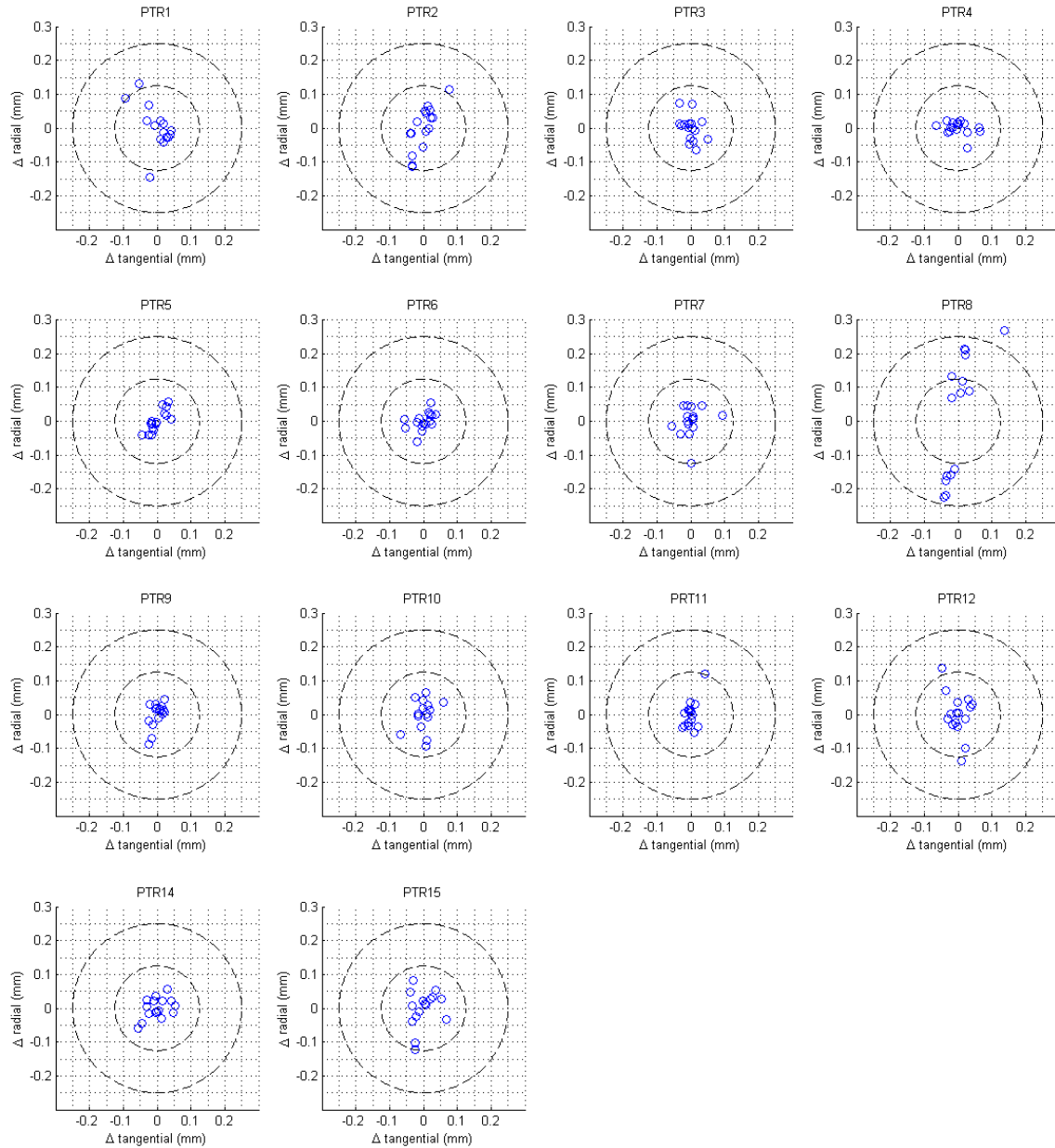


Figure 18. The spread of petal truss ring points over the 16 deployments. Radial and tangential directions are the (r, theta) unit vectors in a polar coordinate system with the nominal occulter center at the origin. Blue circles represent individual deployments. Circles of radius 125 micrometers and 250 micrometers are shown for scale.

5.3 Analysis and application to milestone. The statistical tool we used to check whether we met our milestone was met was a tolerance interval (2). Unlike a confidence interval, which provides confidence bounds on the value of a parameter, a tolerance interval provides confidence bounds on a range of data. For our milestone, we wished to create a tolerance interval such that we are 90% confident it contains 99.73% of the population of future data points. (For a normal distribution, 99.73% of the distribution falls in the mean +/- 3 sigma). The equations and assumptions used to calculate our tolerance interval are further explained in our TDEM report. For brevity, I will not include it here. The resulting tolerance intervals are given graphically in Figure 19.

Figure 19 shows the mean deviation of the 8 petal root points after the 15 deployments with the resulting tolerance intervals, in both the radial and tangential directions. Radial errors show a residual bias that could be reduced with additional shimming. Tangential errors are minimal for the two inner petals and larger but still within the tolerance limit for the two outer petals. This behavior is an expected manifestation of using existing hardware. The petals need to be registered to truss nodes (junction between bays) as they are the only points with precision deployment repeatability. The existing Astromesh antenna provides no registration features to precisely locate the nodal position. A retrofitted registration feature was possible for only the primary nodes, but not the alternating dependent nodes. A registration tool was installed to the primary node between petals 2 and 3 (attach points 4 and 5). A precision tool is used to locate attach points 3 and 6. Attach points on petals 1 and 2 (attach points 1, 2, 7 and 8) are positioned with further extrapolation and the errors start compounding. Future custom designs will include the necessary registration features at every node. Nevertheless, the 90% confidence is well within the milestone requirement of ± 0.95 mm.

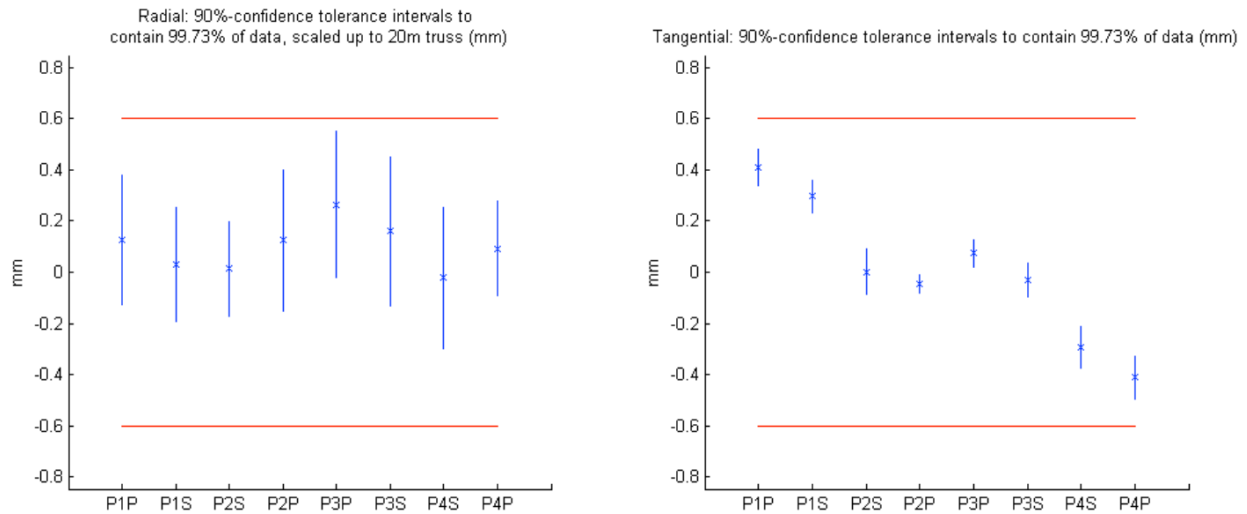


Figure 19. A set of tolerance intervals for the eight petal root points which contain 99.73% of deployments with 90% confidence. *Left.* In the radial direction *Right.* In the tangential direction

6. FINAL REMARKS

Most importantly, our technology demonstration retired a major technology element of Starshade manufacturability in showing that it is possible to achieve the required in-plane tolerance of the petal root positions for a 10^{-9} contrast Starshade. To this point, our as-measured petal root positions were actually commensurate with a 4×10^{-10} contrast Starshade. Focusing on the mechanical requirement, the milestone of ± 0.95 mm, being an absolute position accuracy requirement, is easily achievable to a very small residual mean offset, which was demonstrated by removing most of the radial offset from the theoretical model position with just one iteration of shimming. Future designs would also allow for or eliminate the need for tangential shimming, which would reduce our residual tangential error to nearly zero, which would leave absolute position error to be dominated by repeatability. This is very encouraging because repeatability data, when looked at without its mean residual error component, was extremely good, with most all deployment data in Figures 17 & 18 falling within circles of a diameter of 250 microns, or ± 0.125 mm. Future development work for a Starshade-specific inner disk truss will allow us to design a truss specifically suited for attaching, furl and deploy the Starshade petals and will also focus on in-plane petal position and deployment repeatability, allowing us to do further deployment positional accuracy and repeatability testing and hopefully demonstrate even better Starshade contrast possibility.

This work was carried out at the Jet Propulsion Laboratory, California Institute of Technology, under contract to the National Aeronautics and Space Administration.

7. REFERENCES

- [1] R. J. Vanderbei, E. J. Cady, and N. J. Kasdin. Optimal occulter design for finding extrasolar planets. *Astrophysical Journal*, 665:794{798, 2007.
- [2] G. J. Hahn and W. Q. Meeker. *Statistical Intervals: A Guide for Practitioners*. John Wiley and Sons, Inc., 1991.
- [3] W. A. Jensen. Approximations of tolerance intervals for normally distributed data. *Quality and Reliability Engineering International*, 25(5):571 {580, 2009.
- [4] E. Cady. Boundary diffraction wave integrals for diffraction modeling of external occulter. *Optics Express*, 20:15196{15208, July 2012.
- [5] Stuart B. Shaklan, M. Charley Noecker, Tiffany Glassman, Amy S. Lo, Philip J. Dumont, N. Jeremy Kasdin, Eric J. Cady, Robert Vanderbei, and Peter R. Lawson. Error budgeting and tolerancing of starshades for exoplanet detection. volume 7731, page 77312G. SPIE, 2010.
- [6] Verifying Deployment Tolerances of an External Occulter for Starlight Suppression